mathematics

Article

Direction of Arrival Estimation Method Based on Eigenvalues and Eigenvectors for Coherent Signals in Impulsive Noise

Junyan Cui [1], Wei Pan [1,2] and Haipeng Wang [1,2,3,4,*]

[1] School of Electronics and Information Engineering, Nanjing University of Information Science and Technology, Nanjing 210044, China; 202183270508@nuist.edu.cn (J.C.); 202212490241@nuist.edu.cn (W.P.)
[2] Research Center of Applied Electromagnetics, Nanjing University of Information Science and Technology, Nanjing 210044, China
[3] State Key Laboratory of Millimeter Waves, Southeast University, Nanjing 210096, China
[4] Nanjing Xinda Institute of Safety and Emergency Management, Nanjing 210044, China
* Correspondence: 003551@nuist.edu.cn

Abstract: In this paper, a Toeplitz construction method based on eigenvalues and eigenvectors is proposed to combine with traditional denoising algorithms, including fractional low-order moment (FLOM), phased fractional low-order moment (PFLOM), and correntropy-based correlation (CRCO) methods. It can improve the direction of arrival (DOA) estimation of signals in impulsive noise. Firstly, the algorithm performs eigenvalue decomposition on the received covariance matrix to obtain eigenvectors and eigenvalues, and then the Toeplitz matrix is created according to the eigenvectors corresponding to its eigenvalues. Secondly, the spatial averaging method is used to obtain an unbiased estimate of the Toeplitz matrix, which is then weighted and added based on the corresponding eigenvalues. Next, the noise subspace of the Toeplitz matrix is reconstructed to obtain the one that has less angle information. Finally, the DOA of the coherent signal is estimated using the Multiple Signal Classification (MUSIC) algorithm. The improved method based on the Toeplitz matrix can not only suppress the effect of impulsive noise but can also solve the problem of aperture loss due to its decoherence. A series of simulations have shown that they have better performances than other algorithms.

Keywords: coherent signal; eigenvalue; eigenvector; Toeplitz matrix; DOA estimation; impulsive noise

MSC: 94-10

check for updates

Citation: Cui, J.; Pan, W.; Wang, H. Direction of Arrival Estimation Method Based on Eigenvalues and Eigenvectors for Coherent Signals in Impulsive Noise. *Mathematics* **2024**, *12*, 832. https://doi.org/10.3390/math12060832

Academic Editor: Ke-Lin Du

Received: 12 February 2024
Revised: 10 March 2024
Accepted: 11 March 2024
Published: 12 March 2024

1. Introduction

The direction of arrival (DOA) estimation is an important research direction. The angle information of the target is one of the important parameters that are required by modern communications. DOA information is widely used in radar, sonar, wireless communications, and other fields [1–4]. Therefore, algorithm research on DOA estimation has received widespread attention. Subspace-based DOA estimation methods, such as the Multiple Signal Classification (MUSIC) algorithm [5,6] and Estimating Signal Parameters Via Rotational Invariance Techniques (ESPRIT) algorithm [7–9], provide high resolution for estimating uncorrelated signals. Then, some algorithms [10–12] about compressive sensing are proposed to ensure greater accuracy with a lower number of antennas. However, in the case of coherent signals and impulsive noise, the estimation accuracy of these algorithms decreases due to the rank deficiency of the covariance matrix and noise interference. Hence, addressing the estimation algorithms of the covariance matrix under coherent signals with complex noise has emerged as a contemporary research focus.

For the DOA estimation in the presence of impulsive noise, Tsung-Hsien Liu and Jerry M. Mendel introduced a method [13] employing the fractional low-order moment (FLOM) for signal processing in the context of impulsive noise, aiming to mitigate the impact of impulsive noise. However, it is important to note that this approach is not suitable for DOA estimation when coherent signals are involved. Moreover, the method requires prior information on the characteristic parameters of impulsive noise, which has certain limitations. To address this issue, a novel correntropy-based correlation (CRCO) method [14] is proposed. This approach effectively enhances the accuracy of DOA estimation under impulsive noise, simultaneously demonstrating promising results in Gaussian noise scenarios. However, in practical scenarios, signals often exhibit coherence owing to reflection phenomena, and the methods mentioned above have difficulty in distinguishing such coherent signals.

For the estimation of coherent signals, researchers have proposed many methods. These are mainly divided into two categories, one of which realizes the decoherence of the signal by constructing the Toeplitz matrix [15–17], and the other uses the spatial smoothing method (SS) [18–21]. The Toeplitz matrix is constructed by considering the uniform linear array (ULA) as a symmetric matrix [15], which imposes specific requirements on the number of array elements. In ref. [13], a coprime array is employed to construct a low-rank Toeplitz matrix, aiming to enhance the DOA estimation performance for coherent signals. However, it introduces specific requirements for the distribution of array elements. Moreover, the two methods described above do not take the influence of noise into account. A novel method based on correntropy-based generalized covariance (CEGC) is proposed to construct a Toeplitz matrix [17]. However, it does not take full advantage of the properties of the reception correlation matrix itself because the generation of a Toeplitz matrix involves the diagonal summation of all elements across the matrix, followed by average summation. This process has a partial loss of angular information during the procedure of averaging summation. In addition, the SS method partitions the uniform linear array into multiple overlapping subarrays containing the same number of array elements. The covariance matrix of each subarray is then accumulated and averaged, ultimately resulting in the matrix of the recovered rank. It is widely used and combined with traditional denoising algorithms for the DOA estimation of coherent signals in impulsive noise. But the SS algorithm diminishes the effective aperture of the receiving array, which affects the number of received sources and the resolution of the received signal. Li et al. combined SS with FLOM to solve the DOA estimation problem of coherent signals under impulsive noise despite lacking good estimation accuracy [18]. In response to this, Li and Lin applied SS to the phased fractional low-order moment (PFLOM) to improve the efficiency of DOA estimation [19]. Nevertheless, it also experienced aperture loss, which greatly limited the estimation performance.

In this article, a Toeplitz algorithm based on eigenvalues and eigenvectors is presented to solve the issues mentioned above. First, the algorithm performs eigenvalue decomposition on the received covariance matrix to obtain eigenvectors and eigenvalues. The Toeplitz matrix is subsequently built based on the eigenvectors and eigenvalues. In addition, an unbiased estimate of the Toeplitz matrix is attained using the spatial averaging method, which is then weighted and added according to the corresponding eigenvalues. Then, the noise subspace of the Toeplitz matrix is reconstructed to obtain a new noise subspace. Finally, the DOA of the coherent signal is estimated using the MUSIC algorithm. The proposed algorithm has the following advantages: (1) It provides a perspective to construct the Toeplitz matrix with eigenvectors and eigenvalues. (2) The DOA estimated range and accuracy of applicable denoising algorithms, such as FLOM, PFLOM, and CRCO, can be increased by employing this method. (3) The constructed Toeplitz matrix only requires a uniform linear array, which is beneficial to practical applications.

2. Signal Model

2.1. Received Signal Model

A uniform line array is used, assuming that there are M array elements arranged at equal intervals, where the spacing of the array elements is $\lambda/2$. There are D ($D < M$) coherent signals $s_k(t)$ incident in the array in the form of plane waves, whose wavelengths are λ and angles of incidence are θ_1, θ_2, θ_3, ..., θ_D, respectively. Then, at the moment t, the signal $x_m(t)$ received at the mth array element is given by the following:

$$x_m(t) = \sum_{k=1}^{D} a_m(\theta_k)s_k(t) + n_m(t) \tag{1}$$

where $a_m(\theta_k)$ represents the orientation vector of the k_{th} signal on the m_{th} array element.

The vector form of Equation (1) is given as follows:

$$\mathbf{X}(t) = \mathbf{AS}(t) + \mathbf{N}(t) \tag{2}$$

where $\mathbf{X}(t)$ is the $M \times 1$ dimensional received data vector, $\mathbf{A}$ is the $M \times D$ dimensional array of guide vectors, $\mathbf{S}(t)$ is the $D \times 1$ dimensional signal vector, and $\mathbf{N}(t)$ is the $M \times 1$ dimensional noise vector.

2.2. Coherent Signal Model

The correlation coefficient is commonly employed to characterize the association between signals. A higher correlation coefficient indicates a more substantiated correlation between the two signals. For two correlated signals, $s_i(t)$ and $s_j(t)$, their correlation coefficients z_{ij} are defined as follows:

$$z_{ij} = \frac{E\left[s_i(t)s_j^*(t)\right]}{\sqrt{E\left[|s_i(t)|^2\right]E\left[|s_j(t)|^2\right]}}, |z_{ij}| \leq 1 \tag{3}$$

The correlation of the signals is defined as follows:

$$\begin{cases} z_{ij} = 0, & \text{uncorrelated} \\ 0 < |z_{ij}| < 1, & \text{correlate} \\ |z_{ij}| = 1, & \text{coherent} \end{cases} \tag{4}$$

The coherent signals are modeled as follows:

$$\begin{aligned} \mathbf{X}(t) &= \mathbf{AS}(t) + \mathbf{N}(t) \\ &= \mathbf{A}\begin{bmatrix} 1 \\ \beta_1 \\ \vdots \\ \beta_{D-1} \end{bmatrix} s_0(t) + \mathbf{N}(t) \\ &= \mathbf{AC}s_0(t) + \mathbf{N}(t) \end{aligned} \tag{5}$$

where $\mathbf{C}$ is a column vector of D $\times$ 1 dimensions composed of complex constants, and $s_0(t)$ follows a normal distribution, which is independent of the noise $\mathbf{N}(t)$.

2.3. Impulsive Noise Model

The noise encountered in practical radar applications often has certain impulsive characteristics, such as cosmic noise and atmospheric noise. At this time, the Gaussian distribution is no longer suitable for describing its distribution characteristics. In recent years, a large number of studies [22] have shown that the symmetrical alpha distribution ($S\alpha S$) can be used to describe the distribution characteristics of impulsive noise. Its eigenfunction can be expressed as follows:

$$\varphi(t) = \begin{cases} \exp\{-\sigma^\alpha |t|^\alpha [1 - i\beta(\text{sign}(t))\tan(\pi\alpha/2)]i\mu t\}, \alpha \neq 1 \\ \exp\{-\sigma|t|[1 + i\beta(\text{sign}(t))2/\pi \log|t|]i\mu t\}, \alpha = 1 \end{cases} \tag{6}$$

$$\text{sign}(t) = \begin{cases} 1, & t > 0 \\ 0, & t = 0 \\ -1, & t < 0 \end{cases} \tag{7}$$

where the parameter α is a characteristic parameter, indicating the shock characteristics of the noise. β is the symmetric parameter, which is used to confirm the degree of symmetrical inclination. $\beta = 0$ represents a symmetrical distribution, abbreviated as $S\alpha S$. σ denotes the dispersion coefficient, which is used to describe the degree of dispersion of the sample. μ is the orientation parameter, representing the mean when $0 < \alpha < 1$ and the median when $1 < \alpha < 2$. It should be noted that when $\alpha = 2$, the $S\alpha S$ distribution transitions into a Gaussian distribution. Figure 1 shows the corresponding probability density function (PDF) for different α.

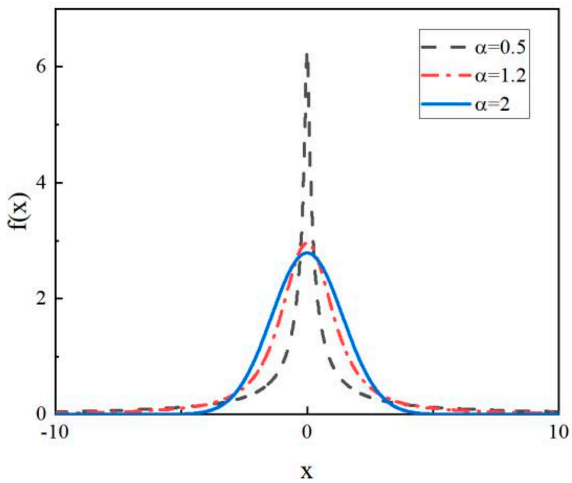

Figure 1. Probability density function curve for different values of α.

According to Figure 1, it can be shown that as the α value decreases, the peak of the PDF curve becomes sharper, the tail is thicker, and the impulsive characteristics of the corresponding distribution become more pronounced.

3. FLOM, PFLOM and CRCO Algorithm

Since the SαS distribution only has limited low-order moments, the traditional algorithm using second-order moments is no longer applicable. Therefore, according to ref. [13], a FLOM matrix is constructed, which is specifically defined as follows:

$$\Gamma_{FLOM}(i,k) = E\{x_i(t)\left|x_k(t)\right|^{2-p}x_k^*(t)\}, 1 < p < \alpha \le 2 \tag{8}$$

where $x_i(t)$, $x_k(t)$ are the outputs of any array element. Moreover, ref. [19] introduces a phased FLOM matrix to solve this problem, and when $\alpha < 1$, it can also reduce the impulsive noise very well.

$$\Gamma_{PFLOM}(i,k) = E\{x_i(t)|x_i(t)|^{a-1}x_k^*(t)|x_k(t)|^{a-1}\}, 1 < a < \frac{\alpha}{2} \tag{9}$$

where * represents the complex conjugate.

In addition, ref. [14] presents a CRCO-based matrix to solve the DOA estimation under the $S\alpha S$ distribution. The specific matrix is as follows.

$$\Gamma_{CRCO}(i,k) = E\{\exp(-\frac{(x_i(t) - \mu x_k(t))^2}{2\sigma^2})x_i(t)x_k(t)\} \tag{10}$$

where μ is given a positive parameter to ensure the corretropy-based autocorrelation is finite. σ is the kernel size that controls the bandwidth of the Correntropy-induced metric (CIM) "mix norm" [23], $\mu = 0.5$, $\sigma = 1.4\sigma_0$, σ_0 is the estimated variance of the signal with no noise.

4. Proposed Method

Firstly, we performed eigenvalue decomposition on the matrix Γ constructed in Section 3.

$$\boldsymbol{\Gamma} = \mathbf{Q}\boldsymbol{\Sigma}\mathbf{Q}^H \tag{11}$$

where $\mathbf{Q}$ and $\boldsymbol{\Sigma}$ are defined as follows:

$$\mathbf{Q} = [u_1, u_2, \ldots, u_{(M-1)}, u_M] \tag{12}$$

$$u_n = [u_{1n}, u_{2n}, \ldots, u_{(M-1)n}, u_{Mn}]^T \tag{13}$$

$$\boldsymbol{\Sigma} = diag\{\lambda_1, \lambda_2, \ldots, \lambda_{(M-1)}, \lambda_M\} \tag{14}$$

and where λ_1,..., λ_M are sorted in descending order.

Secondly, given that the eigenvalues encapsulate the angle information of the incident signal, some eigenvalues are extracted, and their corresponding eigenvectors are employed to construct the Toeplitz matrix. The specific steps are as follows:

- Create the following coherence function:

$$\begin{cases} c_n(k-1) = u_{1n}u_{kn}{}^* \\ c_n(-k+1) = u_{kn}u_{1n}{}^* \end{cases}, k = 1, 2, \ldots, M \tag{15}$$

- Build the Toeplitz matrix with the following coherence function:

$$\mathbf{C_n} = \begin{bmatrix} c_n(0) & \ldots & c_n(M-1) \\ \vdots & \ddots & \vdots \\ c_n(-M+1) & \cdots & c_n(0) \end{bmatrix} \tag{16}$$

- The unbiased estimate of $\mathbf{C_n}$ is calculated by applying forward and backward-averaging terms.

$$\mathbf{C'_n} = \mathbf{C_n} + \mathbf{J}\mathbf{C_n^H}\mathbf{J} \tag{17}$$

$\mathbf{J}$ is shown in Equation (18):

$$\mathbf{J} = \begin{bmatrix} 0 & 0 & \cdots & 0 & 1 \\ 0 & 0 & \cdots & 1 & 0 \\ \vdots & \vdots & \ddots & \vdots & \vdots \\ 0 & 1 & \cdots & 0 & 0 \\ 1 & 0 & \cdots & 0 & 0 \end{bmatrix} \tag{18}$$

- Introduce penalty variable

Since the angle information of the signal contained in each feature vector has a different proportion, the penalty quantities are introduced to generate the following matrix:

$$\begin{cases} \mathbf{Y} = \sum\limits_{n=1}^{P} \sigma_n \mathbf{C}'_n \\ \sigma_n = \left| \frac{\lambda_n}{\sum\limits_{i=1}^{P} \lambda_i} \right| \end{cases} \tag{19}$$

where P is a constant parameter that is positively correlated with the number of signals.

Finally, the noise subspace is extracted from the matrix $\mathbf{Y}$, and the MUSIC algorithm is performed to obtain the DOA. The methods are as follows:

(1) Perform singular value decomposition on $\mathbf{Y}$ to create the noise subspace $\mathbf{W}_1$

$$[\mathbf{U},\mathbf{S},\mathbf{V}] = svd[\mathbf{Y}] \tag{20}$$

where $\mathbf{W_1} = \mathbf{U}(:,D + 1:M)$, $\mathbf{S_1} = \mathbf{S}$, perform the following processing on $\mathbf{S_1}$ to form a rank-deficient receiving covariance matrix.

$$\mathbf{S_1}(M-n, M-n) = 0, n = 0,1,2,\cdots, D-1 \tag{21}$$

(2) The related methods are used to produce a new covariance matrix $\mathbf{Y_1}$ and then attain the noise subspace $\mathbf{W_2}$.

$$\mathbf{Y_1}\mathbf{=}\mathbf{U}\mathbf{S_1}\mathbf{V}^* \tag{22}$$

Then, singular value decomposition on $\mathbf{Y_1}$ is performed.

$$[\mathbf{U_1},\mathbf{S_1'},\mathbf{V_1}] = svd[\mathbf{Y}_1] \tag{23}$$

$$\mathbf{W_2} = \mathbf{U_1}(:, D+1 : M) \tag{24}$$

(3) The weighted average of the noise subspaces obtained in the first and second time is used to obtain a new noise subspace $\mathbf{U_n}$, and a spectral peak search is carried out.

$$\mathbf{U_n} = \frac{1}{2}(\mathbf{W_1} + \mathbf{W_2}) \tag{25}$$

Since the signal subspace is orthogonal to the noise subspace, the spatial spectrum function is created as follows:

$$P_{music}(\theta) = \frac{1}{a(\theta)^H \mathbf{U_n} \mathbf{U_n}^H a(\theta)} \tag{26}$$

The spectral peak is then searched to obtain the incident angle.

5. Experimental Analysis

The decoherence algorithm currently widely used in coherent signals with impulsive noise is the spatial smoothing algorithm. In this section, the proposed algorithm is combined with the FLOM, PFLOM, and CRCO algorithms (FLOM-Toeplitz, PFLOM-Toeplitz, CRCO-Toeplitz). In order to prove its effectiveness, it is compared with FLOM-SS [18], PFLOM-SS [19], and CRCO-SS [24].

Since the variance of impulsive noise, which conforms to the $S\alpha S$ distribution, is unbounded, the generalized signal-to-noise ratio (GSNR) is used to define the ratio of signal power to noise power.

$$\mathrm{GSNR} = 10\log(\frac{E\{|s(t)|^2\}}{\sigma^\alpha}) \tag{27}$$

In order to better evaluate the accuracy of the DOA estimation, the root mean square error (RMSE) is defined as follows:

$$\theta_R = \sqrt{\frac{1}{N}\sum_{i=1}^{N}(\hat{\theta}_i - \theta_i)^2} \tag{28}$$

where N is the number of independent experiments, and $\hat{\theta}_i$ is the estimated angle for the ith experiment.

The simulation parameters of both the signal and the impulsive noise are shown in Table 1.

Table 1. Parameter setting.

Symbol	Meaning	Value
D	Number of signals	3
M	Number of array elements	12
L	Number of sub-array elements	10
θ	Incident angle	$\{60°,30°,0°\}$
β	Symmetry parameters	0
μ	Orientation parameters	0
σ	Dispersion parameter	1
p	FLOM constant	1.2
a	PFLOM constant	0.5
N	Number of experiments	100
P	Constant parameter	3

Some variables are assigned when used.

5.1. Comparison of Spatial Spectra

In order to better assess the performance of the above algorithm, a simulation experiment on spatial spectra was conducted for the incident process of the coherent signal with impulsive noise. In this simulation, GSNR = 15, K = 200 (where K represents the number of snapshots) and $\alpha = 0.9$. The results are shown in Figures 2–4. Compared with the spatial spectrum generated by the SS algorithm, the side lobe heights of the spatial spectrum produced by the presented algorithm can be reduced and have a sharper main lobe. Therefore, we can arrive at the conclusion that the proposed algorithm has a better performance than the SS algorithm.

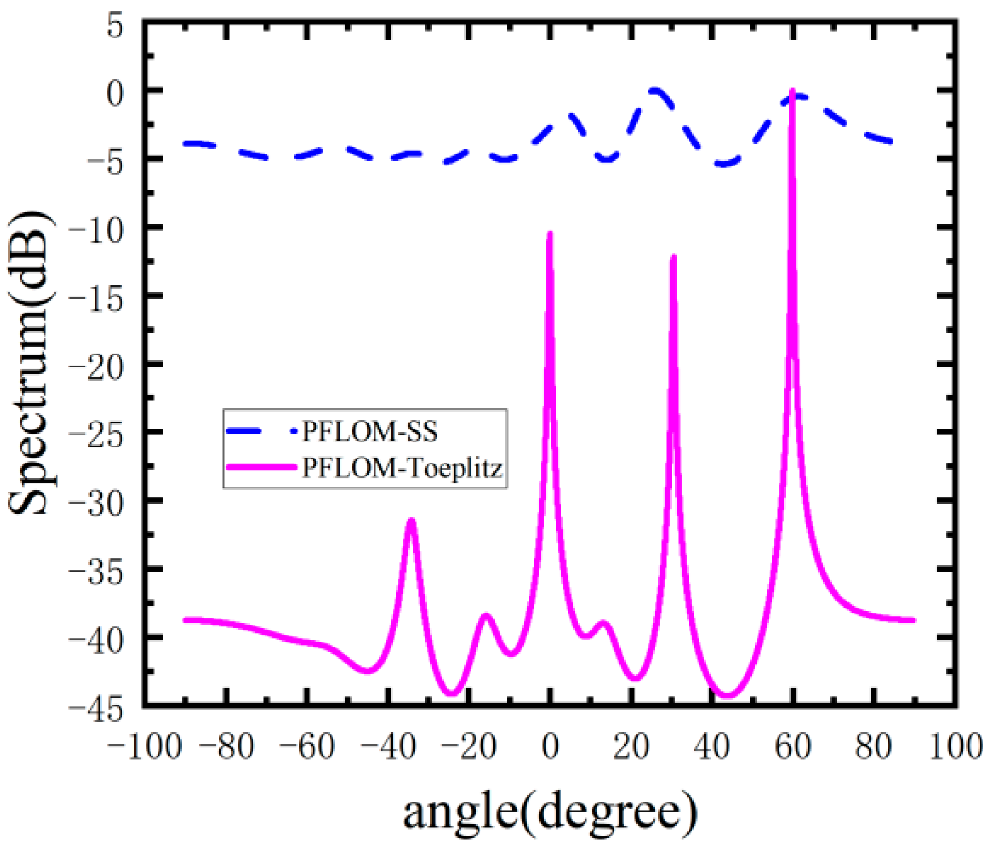

Figure 2. PFLOM-SS's and PFLOM-Toeplitz's spatial spectra.

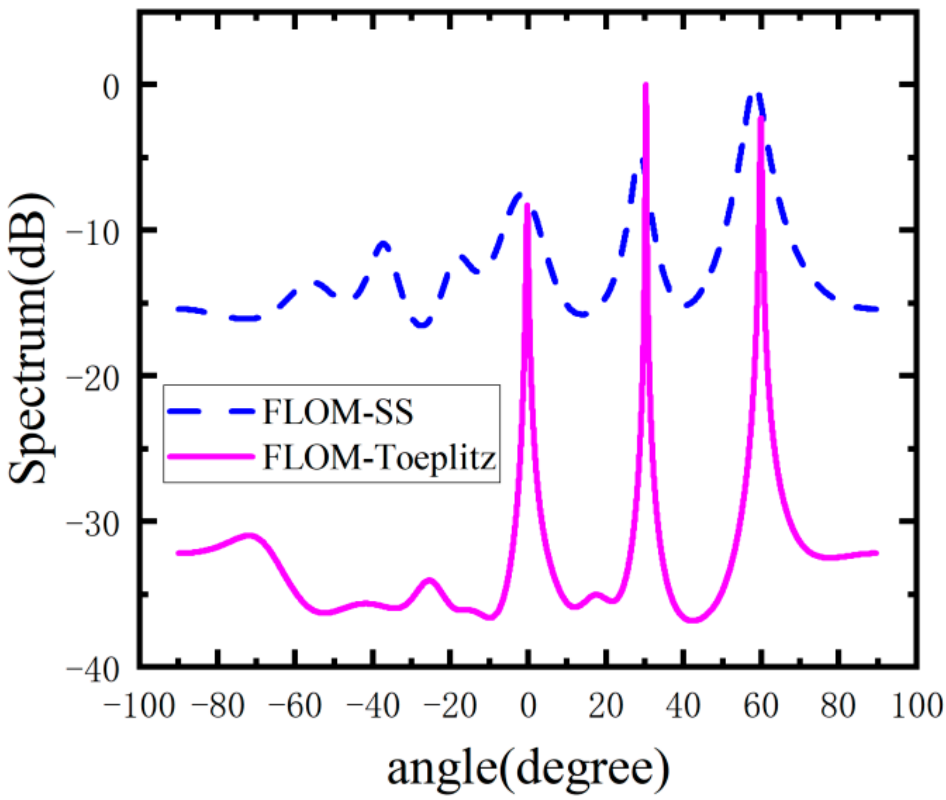

Figure 3. FLOM-SS's and FLOM-Toeplitz's spatial spectra.

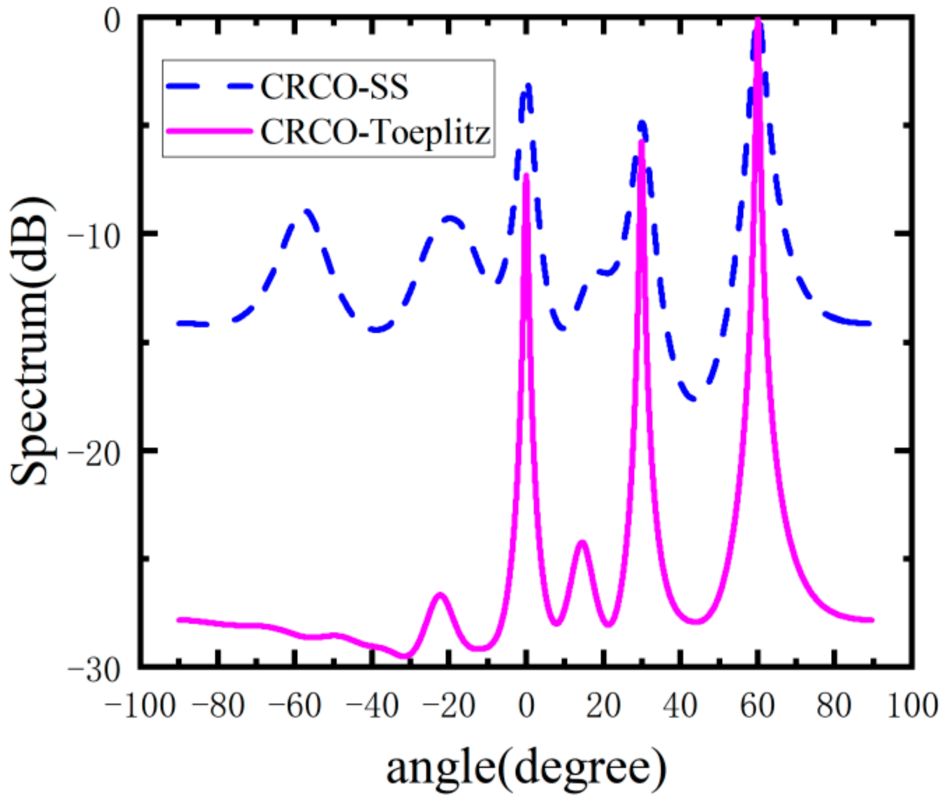

Figure 4. CRCO-SS's and CRCO-Toeplitz's spatial spectra.

5.2. Performance Analysis

This section evaluates the function of the algorithm mentioned above in terms of the snapshot number K, GSNR, and feature vectors and compares the results to show the superiority of the Toeplitz algorithm. In these simulations, GSNR = 20, K = 200, and $\alpha = 1.6$. One of them can be changed while keeping the others unchanged to compare their effectiveness. The results of the algorithm applied to FLOM are shown in Figure 5. The pink curve denotes the proposed algorithm, while the orange curve represents the existing algorithm.

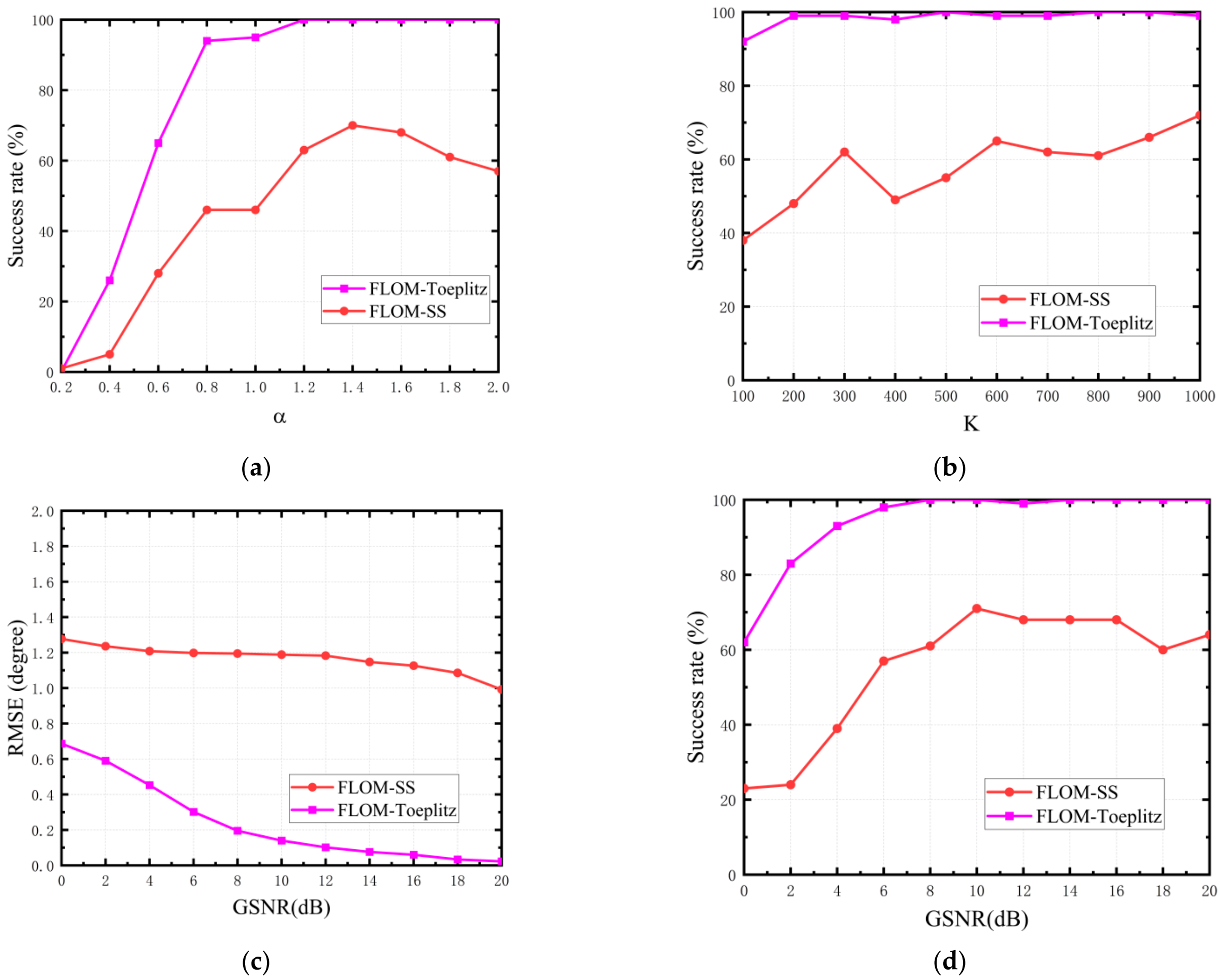

Figure 5. Performance comparison between FLOM-SS and FLOM-Toeplitz. (**a**) Estimated success rate versus α. (**b**) Estimated success rate versus number of snapshots. (**c**) RMSE versus GSNR. (**d**) Estimated success rate versus GSNR.

As illustrated in Figure 5, the estimated success rate of the FLOM-Toeplitz algorithm was greater than that of FLOM-SS under different snapshot numbers, impact characteristics, and GSNR. It can be seen that as the impact characteristics of noise decrease, the estimated success rate of this algorithm gradually increases. When $\alpha > 1.2$, the estimated success rate reaches 100%, while the success rate of FLOM-SS is only 60%. In addition, regardless of the low number of snapshots or the high number of snapshots, the estimated success rate is greater than that of FLOM-SS. Moreover, with different GSNR, the RSME of the FLOM-Toeplitz algorithm is below 0.8°, which is much lower than that of the FLOM-SS algorithm and continues to decrease as GSNR increases. It can be observed that the algorithm is adequately combined with FLOM for the DOA estimation of coherent signals in impact noise. The result of the algorithm applied to PFLOM is shown in Figure 6.

The existing algorithm is represented by the color orange, whereas the proposed algorithm is denoted by the color blue in Figure 6. In Figure 6a, it can be seen that when $\alpha < 1$, the success rate is nearly 0% because the PFLOM constant $a > \alpha/2$ does not satisfy the requirement of Equation (7). When $\alpha > 1$, the success rate of the PFLOM-Toeplitz algorithm increases faster than that of PFLOM-SS. It is easy to know that the success rate of the PFLOM-Toeplitz algorithm has been steadily higher than that of the PFLOM-SS algorithm in Figure 6b. In addition, when GSNR is low, the RMSE of the PFLOM-Toeplitz algorithm is lower than 0.6 (Figure 6c,d). At the same time, the RMSE of the PFLOM-SS algorithm is nearly 1.0. Meanwhile, the success rate of the PFLOM-Toeplitz algorithm (above 70%) is significantly higher than that of PFLOM-Toeplitz under a low GSNR. It is indicated that this algorithm can be well combined with PFLOM for the DOA estimation of coherent signals with impulsive noise.

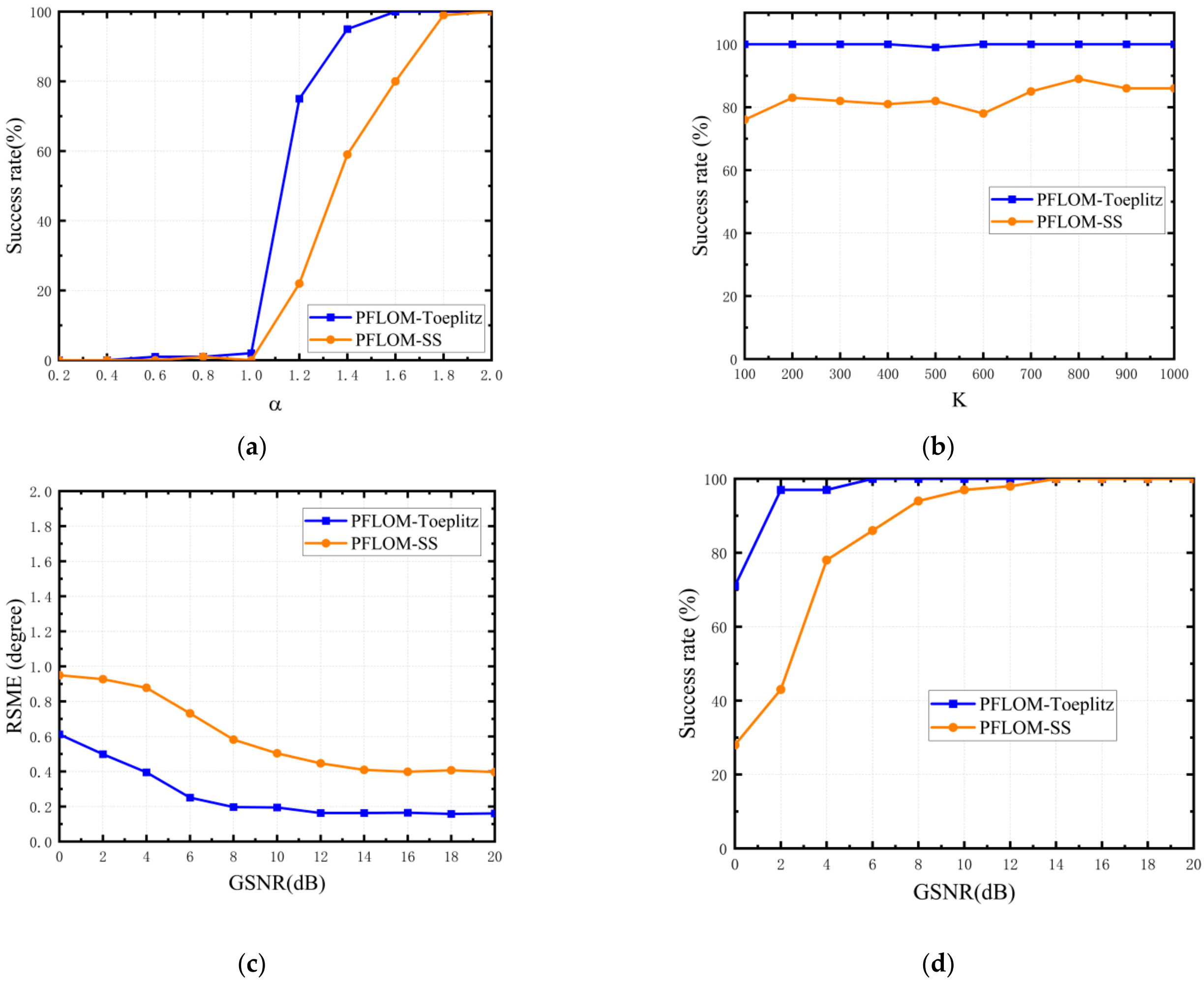

Figure 6. Performance comparison between PFLOM-SS and PFLOM-Toeplitz. (**a**) Estimated success rate versus α. (**b**) Estimated success rate versus number of snapshots. (**c**) RMSE versus GSNR. (**d**) Estimated success rate versus GSNR.

The result of the algorithm applied to CRCO is shown in Figure 7. The color blue represents the proposed algorithm, while the color orange is used to denote the existing algorithm. It can be clearly seen that the CRCO-SS and CRCO-Toeplitz algorithms both have a good estimation for a large range of α (Figure 7a). In addition, the estimation accuracy at low snapshots is effectively improved in Figure 7b. The success rate of the CRCO-Toeplitz algorithm is above 90%, while that of the CRCO-SS algorithm is only about 70%. At the same time, RMSE is reduced over the entire range of GSNR (Figure 7c). Furthermore, the success rate is also slightly improved in Figure 7d).

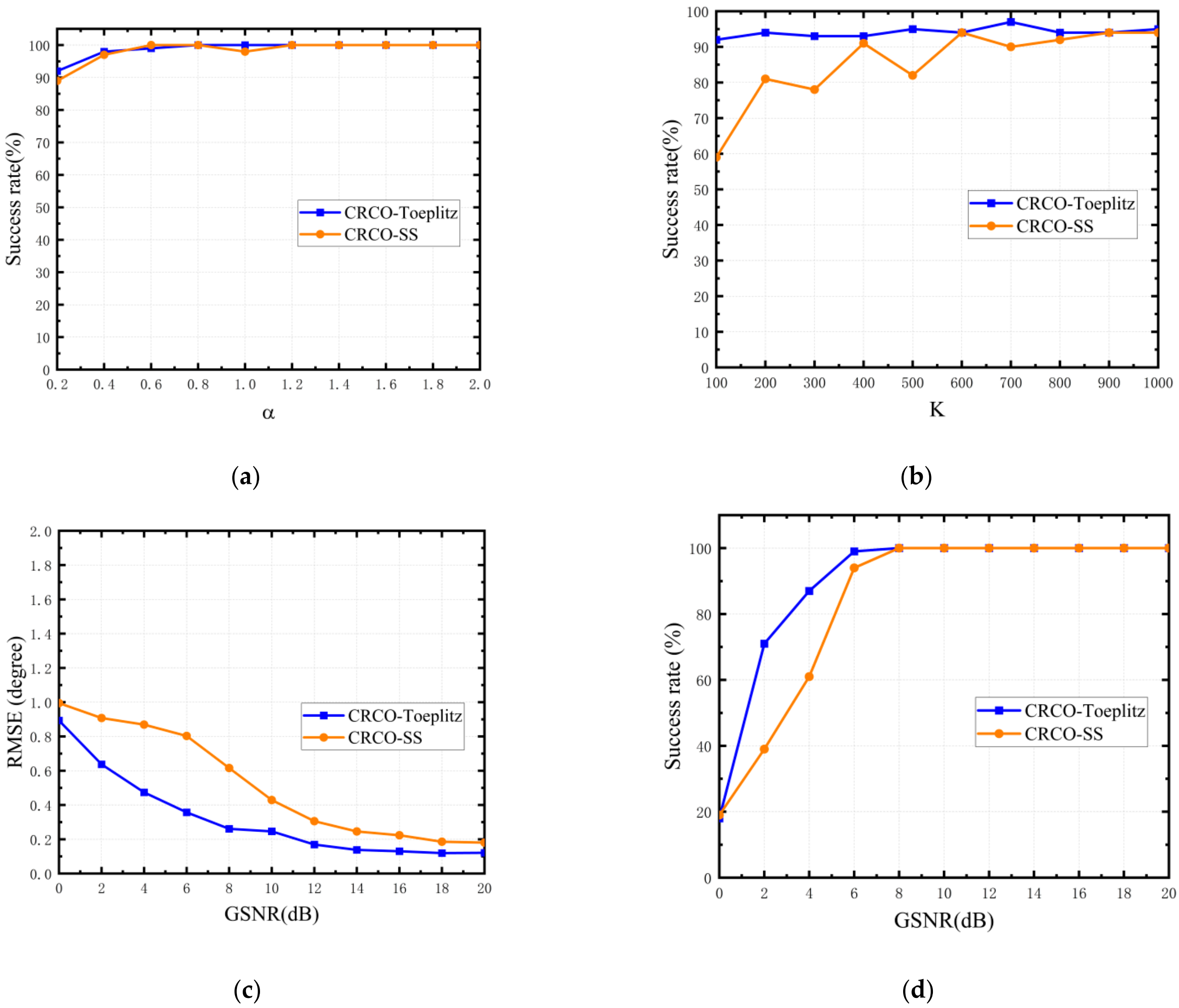

Figure 7. Performance comparison between CRCO-SS and CRCO-Toeplitz. (**a**) Estimated success rate versus α. (**b**) Estimated success rate versus number of snapshots. (**c**) RMSE versus GSNR. (**d**) Estimated success rate versus GSNR.

5.3. Compared with the Exiting Algorithms

To solve the DOA estimation of coherent signals, some related algorithms [17,25,26] based on correntropy were proposed. In this section, the proposed algorithms were compared to the algorithms proposed in the Ref. [17]. In this simulation, K = 200, $\alpha = 1.1$, and GSNR = 10. The results are shown in Figures 8 and 9.

In Figure 8, the pink curve denotes the proposed algorithm, while the orange curve represents the existing algorithm. When GSNR < 0, the success rate of both algorithms is nearly 0. It can be seen that the proposed algorithm's success rate increases faster than the compared algorithms after GSNR > 0. As soon as GSNR reaches 8 dB, the algorithms can both estimate successfully. In Figure 9, the existing algorithm is represented by the color blue, whereas the proposed algorithm is denoted by the color orange. When the impulse character of noise is high, the success rate of the proposed algorithm is above 90%, while the compared algorithms' success rate is lower than 80%. In addition, with the increase in the value of alpha, the success rate of both algorithms is nearly 100%.

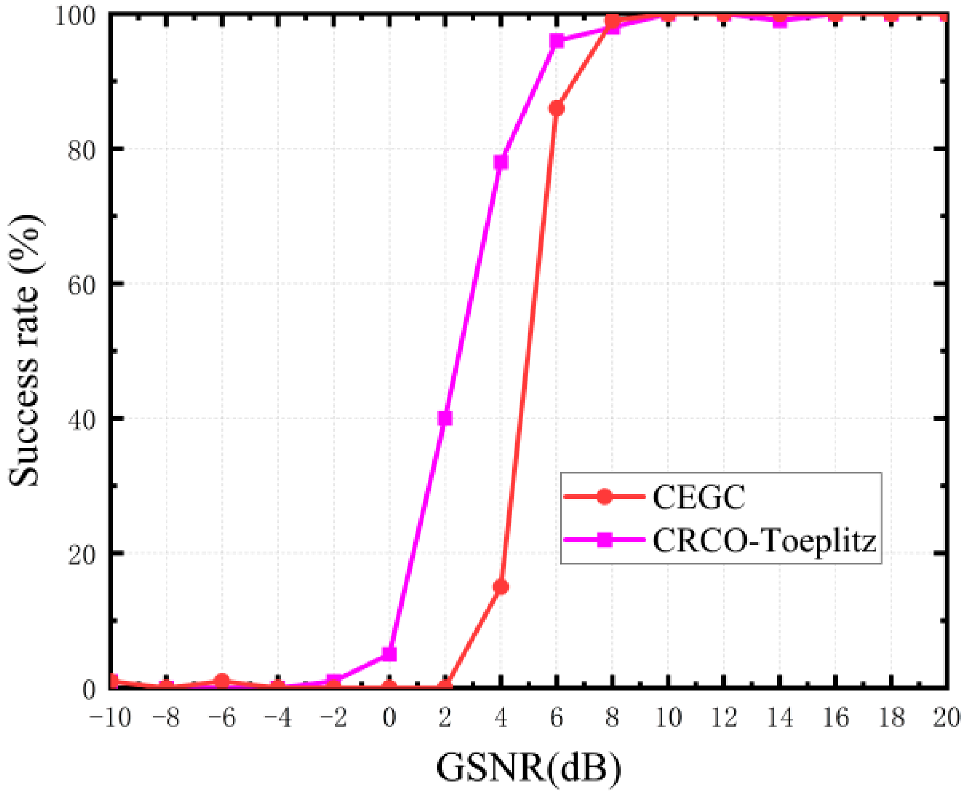

Figure 8. Estimated success rate versus GSNR.

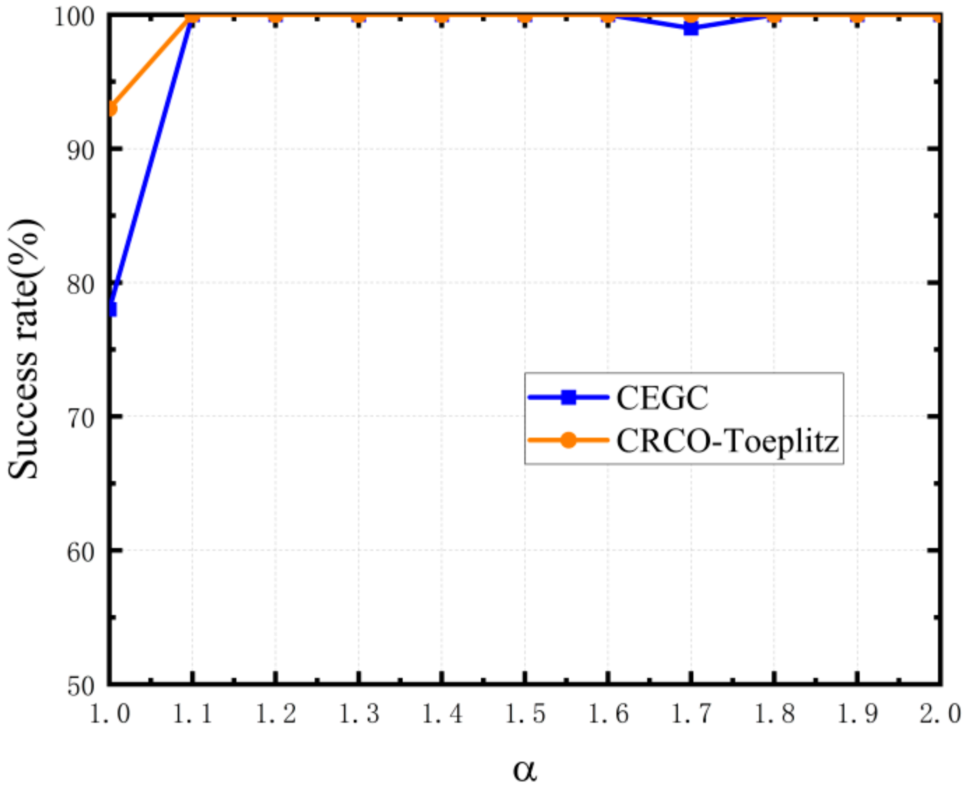

Figure 9. Estimated success rate versus α.

6. Discussions

From the experiments, it can be seen that, compared with the SS algorithm, the proposed Toeplitz algorithm can be used to assist many denoising algorithms, such as FLOM, PFLOM, and CRCO, with the better DOA estimation of coherent signals in the background of impulsive noise. Moreover, the proposed algorithm has a higher accuracy of DOA estimation in a low GSNR and alpha than the compared algorithm.

However, the number of eigenvalues selected in this article is based on the sign sources whose number has been set. When the number of signal sources is not very large, three eigenvalues and eigenvectors are enough to contain all the information of the signal. In situations where there are a large number of signal sources, the proposed algorithm may exhibit inferior accuracy in the DOA estimation. At this time, the proposed algorithms can choose more than three eigenvalues and eigenvectors to construct the Toeplitz matrix.

7. Conclusions

In this paper, an algorithm based on the Toeplitz matrix, which is built by eigenvalues and eigenvectors, is proposed for the improvement of DOA estimation in coherent signals with impulsive noise. At first, the algorithm applies eigenvalue decomposition on the covariance matrix to obtain the eigenvectors and eigenvalues. Then, the Toeplitz matrix is created according to the eigenvectors corresponding to its eigenvalues. Moreover, the spatial averaging method is used to obtain an unbiased estimate of the Toeplitz matrix, which is then weighted and added according to the corresponding eigenvalues. Finally, Toeplitz's subspace is reconstructed, and the MUSIC algorithm is adopted to obtain the DOA estimation. The performance of the proposed algorithm combined with FLOM, PFLOM, and CRCO is verified by the simulation, which proves that it can greatly improve the accuracy of the DOA estimation of coherent signals under impulsive noise.

Future work will focus on improving the accuracy and reliability of the DOA estimation of coherent signals in impulsive noise. Meanwhile, the DOA estimation of an unknown number of coherent sources on impulse is needed, which is a large challenge in real applications. Furthermore, it was better to construct a function to connect the predicted number of coherent sources with the value of the constant parameter P in this future study.

Author Contributions: Conceptualization, J.C.; methodology, J.C.; software, J.C.; validation, H.W.; formal analysis, J.C.; investigation, W.P.; writing—original draft preparation, J.C.; writing—review and editing, H.W.; visualization, W.P.; project administration, H.W.; funding acquisition, H.W. All authors have read and agreed to the published version of the manuscript.

Funding: This research was supported in part by National Natural Science Foundation of China (61801262), Open Research Program of State Key Laboratory of Millimeter Waves (K202312), and the Startup Foundation for Introducing Talent of NUIST (2022r071).

Data Availability Statement: The data presented in this study are available on request from the corresponding author.

Conflicts of Interest: The authors declare no conflicts of interest.

References

1. Chen, Y.; Yang, M.; Li, J.; Zhang, X. A Nested–Nested Sparse Array Specially for Monostatic Colocated MIMO Radar with Increased Degree of Freedom. *Sensors* **2023**, *23*, 9230. [CrossRef] [PubMed]
2. Song, Y.; Zheng, G. Height Measurement for Meter Wave Polarimetric MIMO Radar with Electrically Long Dipole under Complex Terrain. *Remote Sens.* **2023**, *15*, 1265. [CrossRef]
3. Du, L.; Li, H.; Wang, L.; Lin, X.; Lv, Z. Research on High Robustness Underwater Target Estimation Method Based on Variational Sparse Bayesian Inference. *Remote Sens.* **2023**, *15*, 3222. [CrossRef]
4. Mondal, D. Studies of Different Direction of Arrival (DOA) Estimation Algorithm for Smart Antenna in Wireless Communication. *Int. J. Electron. Commun. Technol. IJECT* **2013**, *4*, 47–51.
5. Zhou-hua, Z. The Fourth Order Cumulants Based Modified MUSIC Algorithm for DOA in Colored Noise. In Proceedings of the 2010 Asia-Pacific Conference on Wearable Computing Systems, Shenzhen, China, 17–18 April 2010; pp. 345–347.

6. Vallet, P.; Mestre, X.; Loubaton, P. Performance Analysis of an Improved MUSIC DoA Estimator. *IEEE Trans. Signal Process.* **2015**, *63*, 6407–6422. [CrossRef]
7. Herzog, A.; Habets, E.A.P. Eigenbeam-ESPRIT for DOA-Vector Estimation. *IEEE Signal Process. Lett.* **2019**, *26*, 572–576. [CrossRef]
8. Wu, Y.; Amir, L.; Jensen, J.R.; Liao, G. Joint Pitch and DOA Estimation Using the ESPRIT Method. *IEEE/ACM Trans. Audio Speech Lang. Process.* **2015**, *23*, 32–45. [CrossRef]
9. Lin, J.; Ma, X.; Yan, S.; Hao, C. Time-Frequency Multi-Invariance ESPRIT for DOA Estimation. *IEEE Antennas Wirel. Propag. Lett.* **2016**, *15*, 770–773. [CrossRef]
10. Guo, M.; Zhang, Y.D.; Chen, T. DOA Estimation Using Compressed Sparse Array. *IEEE Trans. Signal Process.* **2018**, *66*, 4133–4146. [CrossRef]
11. Ganguly, S.; Ghosh, J.; Kumar, P.K.; Mukhopadhyay, M. An Efficient DOA Estimation and Jammer Mitigation Method by Means of a Single Snapshot Compressive Sensing Based Sparse Coprime Array. *Wirel. Pers. Commun.* **2022**, *123*, 2737–2757. [CrossRef]
12. Srinivas, K.; Ganguly, S.; Kishore Kumar, P. Performance Comparison of Reconstruction Algorithms in Compressive Sensing Based Single Snapshot DOA Estimation. *IETE J. Res.* **2022**, *68*, 2876–2884. [CrossRef]
13. Liu, T.-H.; Mendel, J.M. A Subspace-Based Direction Finding Algorithm Using Fractional Lower Order Statistics. *IEEE Trans. Signal Process.* **2001**, *49*, 1605–1613. [CrossRef]
14. Zhang, J.; Qiu, T.; Song, A.; Tang, H. A Novel Correntropy Based DOA Estimation Algorithm in Impulsive Noise Environments. *Signal Process.* **2014**, *104*, 346–357. [CrossRef]
15. Zhang, W.; Han, Y.; Jin, M.; Qiao, X. Multiple-Toeplitz Matrices Reconstruction Algorithm for DOA Estimation of Coherent Signals. *IEEE Access* **2019**, *7*, 49504–49512. [CrossRef]
16. Liu, S.; Mao, Z.; Zhang, Y.D.; Huang, Y. Rank Minimization-Based Toeplitz Reconstruction for DoA Estimation Using Coprime Array. *IEEE Commun. Lett.* **2021**, *25*, 2265–2269. [CrossRef]
17. Dai, J.; Qiu, T.; Luan, S.; Tian, Q.; Zhang, J. An Improved Toeplitz Approximation Method for Coherent DOA Estimation in Impulsive Noise Environments. *Entropy* **2023**, *25*, 960. [CrossRef]
18. Li, H.; He, Y.; Wang, H.; Yang, R. Novel Approaches for DOA Estimation of Coherent Sources in the Presence of Impulsive Noise. In Proceedings of the 2006 CIE International Conference on Radar, Shanghai, China, 16–19 October 2006; pp. 1–4.
19. Li, S.; Lin, B. On Spatial Smoothing for Direction-of-Arrival Estimation of Coherent Signals in Impulsive Noise. In Proceedings of the 2015 IEEE Advanced Information Technology, Electronic and Automation Control Conference (IAEAC), Chongqing, China, 19–20 December 2015; pp. 339–343.
20. Hou, Y.; Wang, X.; Ding, L.; Jin, X.; Zhang, Q. DOA-Estimation Method Based on Improved Spatial-Smoothing Technique. *Mathematics* **2024**, *12*, 45. [CrossRef]
21. Du, W.; Kirlin, R.L. Improved Spatial Smoothing Techniques for DOA Estimation of Coherent Signals. *IEEE Trans. Signal Process.* **1991**, *39*, 1208–1210. [CrossRef]
22. Nikias, C.L.; Shao, M. *Signal Processing with Alpha-Stable Distributions and Applications*; Wiley-Interscience: Hoboken, NJ, USA, 1995.
23. Santamaria, I.; Pokharel, P.P.; Principe, J.C. Generalized Correlation Function: Definition, Properties, and Application to Blind Equalization. *IEEE Trans. Signal Process.* **2006**, *54*, 2187–2197. [CrossRef]
24. Guan, S.; Chen, J.; Li, K.; Zhao, Y. General Correntropy Based DOA Estimation for Coherent Source with Impulsive Noise. In *Proceedings of 2019 Chinese Intelligent Systems Conference*; Jia, Y., Du, J., Zhang, W., Eds.; Springer: Singapore, 2020; pp. 159–167.
25. Tian, Q.; Qiu, T.; Ma, J.; Li, J.; Li, R. A Simplified DOA Estimation Method Based on Correntropy in the Presence of Impulsive Noise. *IEEE Access* **2018**, *6*, 67010–67025. [CrossRef]
26. Liu, Y.; Wu, Q.; Zhang, Y.; Gao, J.; Qiu, T. Cyclostationarity-Based DOA Estimation Algorithms for Coherent Signals in Impulsive Noise Environments. *J. Wirel. Commun. Netw.* **2019**, *2019*, 81. [CrossRef]